Published in STLE *Tribology Transactions* (Vol. 50, No. 1/January-March 2007, pp. 114-126). Presented at the STLE Annual Meeting in Calgary, Alberta, Canada, May 7-11, 2006.Final manuscript approved Oct. 4, 2006. Review led by Waldek Dmochowski .

Experimental Identification of Bearing Dynamic Force Coefficients in a Flexible Rotor—Further Developments

Oscar De Santiago (STLE member), Dresser-Rand Co., Olean, N.Y. and Luis San Andrés (STLE Fellow), Texas A&M University, College Station, Texas

Editor's Note: This month's Editor's Choice paper includes two subjects—the one captured in the title and the other unspoken. In this paper entitled, "Experimental Identification of Bearing Dynamic Force Coefficients in a Flexible Rotor—Further Developments," the authors Oscar De Santiago and Luis San Andrés discuss a method to predict bearing characteristics based upon experimental measurements taken on a rotating shaft that has been intentionally unbalanced. This type of work is necessary to prove the safety and robustness of such systems. It makes for an interesting read. I, however, prefer the subtler story written between the lines. The hidden subject centers around what happens when a professor's student leaves the university and heads out into industry. Here, professor San Andrés and his graduate student developed a way to model such systems, and published their results in several papers. The student then graduated and tried to apply the new methods in real systems on the plant floor and in the field, only to learn that it is easier to make changes to a rig in the university lab than to a multimillion dollar compressor in the field. The former student rekindles his relationship with the professor, who now has a new crop of students, to devise a way to modify the old technique to allow a safe and practical way to probe real machines on the path to commercialization. This paper shows two things. One is a technique to improve rotating systems. The second is that the teacher-student relationship often lasts much longer than the planned course curriculum and over time it becomes more difficult to see who is the student and who is the teacher. I enjoyed reading this paper and I hope you will as well.

– Dr. Christopher DellaCorte,TLT editor

Nomenclature

D_b, L_b, C_b	= two lobe bearing diameter, length and clearance (m)
D_d, L_d, M_d	= diameter, length (m), and mass (kg) of test rotor disks
D_s, L_s, M_s	= diameter, length (m), and mass (kg) of test rotor shaft
E, ρ_s	= shaft elastic modulus (Pa) and material density (kg/m³)
I	= imaginary unit
$K_{\alpha\beta}$, $C_{\alpha\beta}$,	= bearing support stiffness and damping coefficients (N/m, Ns/m) $\alpha\beta = x,y$
L_1 , L_2	= axial location of test rotor disks (m)
m, u, ϕ	= imbalance mass (kg), imbalance displacement (m), and phase angle (rads)
r_d	= radius of attachment of imbalance mass (m)
s_1 , s_2	= axial location of sensors from the bearing centerline (m)
t	= time (s)
(x,y)	= rotor radial displacement coordinates, horizontal and vertical (m)
Ω	= rotor speed (rad/s)
ω	= excitation frequency (rad/s)

Vectors/matrices

DM	= matrix of measured displacements
$\mathbf{f_B}$	= rotor forces (N) at support locations
$\mathbf{H_B}$	= bearing support impedance matrix (N/m)
$\mathbf{H_R}$	= rotor impedance (dynamic stiffness) matrix (N/m)
$\mathbf{H_{Rab}}$ a,b=1,2,3	= partitions of rotor impedance matrix $\mathbf{H_R}$ (N/m)
M, K, C, G	= global (rotor) mass, stiffness, damping and gyroscopic matrices
Q, q	= vectors of generalized forces and rotor displacements
RF	= reactive force matrix
$\mathbf{z_B}$	= complex radial rotor displacements at supports (m)
$\mathbf{z_u}$	= complex radial rotor displacements (m)

Subindices

B_1, B_2	= bearings supports, 1 and 2
R	= rotor
x,y	= main directions (horizontal and vertical)
u	= locations on the rotor different from bearing locations
j	= linearly independent test case, 1 and 2
k	= imbalance plane axial location, 1 and 2
m	= location of measurement

Keywords

Vibration; Dynamic Modeling; Expert Systems; Condition Monitoring; Maintenance; Data Acquisition Methods; Vibration in Hydrodynamic Lubrication; Journal Bearings; Multi-Lobe Bearings

Abstract

Bearing force coefficients are a necessary component in the analysis of linear stability and response of rotating dynamic systems. Often, these bearing parameters are predicted using limited or restrictive flow models, or operating conditions in the actual machine differ largely from the assumed conditions during the analysis. In these instances, identification of actual support properties represents a means to verify the rotordynamic predictions. The current work presents an identification procedure that is suitable for implementation in the field and that relies on measurements of rotor synchronous response to calibrated imbalance. The method is extended to the typical case when the displacement measurements occur away from the bearing locations in flexible rotor systems. Measurements and identification are performed on a test rotor supported on a pair of identical two-lobe fluid film bearings and for increasing values of imbalance over a speed range from 1,000 to 4,000 rpm. Identification using increased imbalances reveals the linear region of response in which the procedure renders reliable results. Also, a signal noise study shows that the method is robust to random external disturbances with a noise-to-signal ratio of up to 10%.

Introduction

The operation of critical rotating machinery in industrial environments demands of accurate predictions of system dynamic behavior to guarantee reliability and minimize risks. Stringent industrial specifications require verification of predicted response (and in the near future of stability margin) of rotor-bearing systems essential to key production processes.[1-4] Although the controlled imbalance response measurements commonly performed during shop testing provide information about the rotating system critical speed and amplification factors, it is often desirable to confirm the support rotordynamic properties in the test stand and in the field, giving rise to the need for appropriate identification methods. Such methods prove useful for verification of bearing properties prediction as well as for eventual condition monitoring and troubleshooting.

Experimental identification of bearing impedances requires measurements of the rotor response and force excitation. Bearing impedances are complex functions, with real parts representing dynamic stiffnesses and imaginary parts being proportional to the viscous damping coefficients. Goodwin[5] reviews experimental techniques for identification of bearing impedances and classifies them in terms of the type of measuring equipment required, time available to carry out the testing and the reliability of the results. Goodwin concludes that measurements made using multi-frequency test signals provide more reliable data. Most of the methods mentioned are applied in the time-domain and at a particular excitation frequency.

Excitation sources such as harmonic forces, pseudo-random periodic force excitation, rotor imbalance, and impulse loads allow estimation of the bearing impedance functions. Morton[6] uses electromagnetic shakers to apply a sinusoidal excitation to a test journal bearing and measures receptance frequency response functions resulting from unidirectional loading. Practical difficulties arise in exciting a rotating shaft by an external harmonic force.

Transient loading of rotor-bearing systems (impact loading) represents another source of excitation for bearing parameter identification. An impulse excitation covers a wide frequency range, thereby increasing the reliability of the estimated bearing coefficients. Nordmann and Schollhorn[7] present a method in which a rigid rotor supported on journal bearings is excited by a hammer (impulse testing). Recorded forces and displacements of the rotor are transformed into the frequency domain, and then complex frequency response functions are derived. The analytical frequency response functions, which depend on the bearing coefficients, are fitted to the measured functions. The resulting stiffness and damping coefficients correlate well when compared to predictions. De Santiago and San Andrés[8] extends this experimental technique to identify frequency-dependent bearing force coefficients from measured rotor responses due to impact loads at constant running speed. The work includes a study on the variability of estimated parameters due to the number of impacts exerted on the test system.

Another simple excitation load is due to calibrated imbalances distributed at recorded angular and radial locations on a test rotor. This type of excitation is very attractive to industrial practice due to its simplicity and ease of implementation in an assembled machine. Burrows and Sahinkaya[9] identified squeeze film dynamic force coefficients from synchronous excitation, but failed to identify all the force coefficients. In most cases, the estimation procedure depends on the test signal being more significant compared to the inherent imbalance distribution in the system. Lee and Hong[10] present a novel method for identifying bearing dynamic force coefficients by using imbalance measurements, though confining the procedure to a rigid rotor. The procedure also fails for isotropic bearings since the identification matrix encounters a singularity. De Santiago and San Andrés[11] present a procedure that allows identification of synchronous

CONTINUED ON PAGE 44

CONTINUED FROM PAGE 43

bearing parameters from recorded rotor responses to calibrated imbalance mass distribution. The identification procedure requires a minimum of two linearly independent imbalance tests for identification of force coefficients from two bearing supports. Further experimental identification shows the robustness of the method, also restricted to rigid rotors.

Most industrial rotors are flexible and nonsymmetrical. Flexible rotor-bearing systems have been analyzed by many different mathematical methods. In practice, the two most common modeling techniques for slender shafts are the transfer matrix and the finite element method. Ruhl and Booker[12] introduce the finite element method (FEM) for rotor-dynamic analysis. Nelson and McVeigh[13] also present a formulation for dynamic modeling of the rotor-bearing system using distributed parameter finite rotor elements and including rotary inertia, gyroscopic moments and axial load using a consistent mass approach. Zorzi and Nelson[14] generalize this work to include internal viscous and hysteric damping. Nelson[15] extends the previous works by utilizing Timoshenko beam theory to derive shape functions for the beam element, thereby including transverse shear effects. Chen and Lee[16] use FEM for flexible rotors and obtain imbalance responses at two close speeds to identify the bearing coefficients of ball bearings. However, this method requires measurements of response at all nodal points of the shaft model.

The system of equations of motion generated by imbalance excitation tends to be ill-conditioned and most experimental identifications show considerable scatter of results.[17-18] Despite these limitations, the method is suitable for implementation on-site if an appropriate data acquisition system is available. This is typical of many high-performance turbomachines used in critical processes, where the approach is most appealing due to the large amount of standard instrumentation used for machine protection. An identification program can directly take the responses from the data acquisition system and render the bearing synchronous force coefficients.

Yang and Chaung[19] developed an identification method using receptance matrices of flexible shafts from FEM modeling and imbalance forces of trial masses to derive displacements and reaction forces at the bearing locations. The authors introduce a total least squares (TLS) procedure to identify eight bearing coefficients, and show that the method handles noise effectively. San Andrés and De Santiago[20] presented a procedure for identifying bearing support force coefficients in flexible rotor-bearing systems. The identification algorithm models the rotor using a Finite Element Method. The procedure can estimate synchronous force coefficients at a specific operating speed, which makes it suitable for measurements in hydrodynamic bearings showing speed-dependent characteristics.

Most of the identification methods developed[19-20] for flexible rotor-bearing systems require imbalance response measurements at the mid-plane of the bearing locations, which are hard to obtain in actual systems. A scheme for an identification method to work with recorded rotor responses obtained away from the bearing locations is hereby proposed and tested. An investigation on the effects of various parameters that may affect the identification accuracy is also performed. An application is given for a test rotor supported on hydrodynamic journal bearings.

For further details on the various modern methods of identification for bearing force coefficients, time or frequency domain based, the reader should consult the excellent review paper of Tiwari et al.[21]

Figure 1. Test rig for identification of bearing support parameters showing location of displacement sensors, direction of rotation, and details of test rotor geometry.

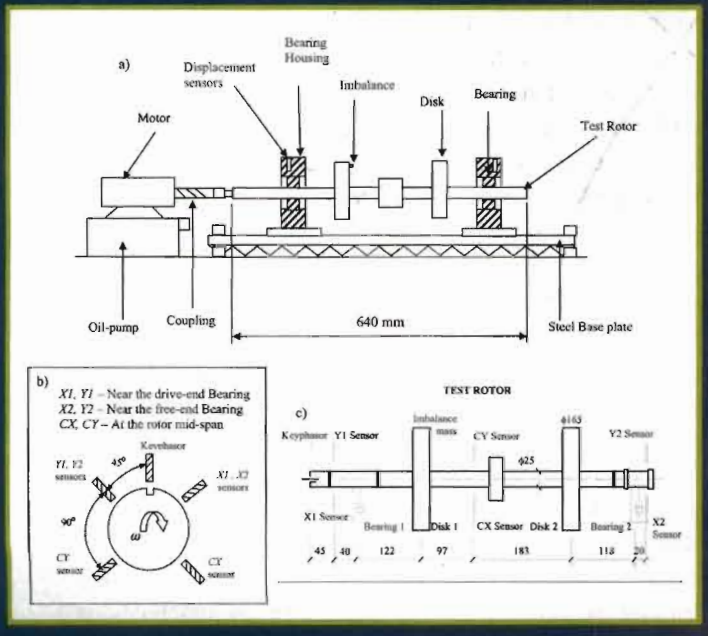

Test rig description and instrumentation

The test rig consists of a slender shaft supported on a pair of two-lobe cylindrical bearings. The shaft has three annular inserts for locating rigid disks enabling the rotor to render different configurations. Figure 1 shows the rig with a two-disk symmetric rotor arrangement. A DC variable speed motor drives the rotor by means of a flexible coupling up to a speed of 8,000 rpm. The bearings are mounted on aluminum housings, which are in turn fixed to a steel base plate.

The steel shaft is 640 mm long with a main diameter of 25.4 mm. Up to four massive disks can be mounted on

the rotor. For the experiments presented herein, two disks, 31.8 mm wide and 165 mm in diameter, are mounted on the shaft 280 mm apart from each other. Each disk weighs 3.86 kg. Threaded holes spaced at 15^0 apart on both sides of each disk serve for placement of imbalance weights. The disks are clamped to the shaft by means of semi-circular plates and bolts.

The test bearings are identical, two-lobe fluid film bearings split horizontally for their easy installation. The bearings are made of bronze with a Babbitt liner. The bearings are lubricated with ISO VG 10 turbine oil. An oil pump delivers the oil through the pipelines into the bearing housing through rectangular grooves machined at the partition line. A valve in the pump discharge line controls the inlet pressure, measured by a pressure gauge. The temperature of the lubricant entering the bearing housings can be controlled by a built-in heater inside the test rig. Table 1 presents the specifications of the rotor-bearing system. For the experiments presented, the inlet pressure of the lubricant is 0.42 bar.

Three pairs of eddy current displacement sensors, orthogonally positioned, record the rotor displacements near each bearing location. Figure 1 shows the angular positioning of the displacement sensors and a description of their axial location (drive-end bearing, free- end bearing, and mid-span). An additional eddy-current displacement sensor, vertically mounted at the shaft end senses a keyway while the rotor spins and provides a reference signal for measuring the shaft speed and phase angles of synchronous response.

Signals from the displacement sensors are directed to an industrial-type data acquisition system connected to a PC computer. An analog oscilloscope is also connected to display the unfiltered real time orbit. The data acquisition system used for measurements has a built-in feature that vectorially compensates the remnant imbalance from measurements.

Figure 1 also depicts the test rotor configuration, with axial locations of the displacement sensors and disks noted. Identification of bearing synchronous force coefficients is performed on the flexible rotor by measuring the synchronous response from calibrated imbalance mass distributions placed at known locations around the circumference of the disks. Three cases of calibrated imbalance masses are chosen. Two linearly independent tests are conducted for each set of imbalance mass distribution to identify all sixteen bearing force coefficients (eight at each bearing location).

Rotor model verification and imbalance response measurements

Free-free natural frequencies of the test rotor are measured by hanging the rotor from two long vertical ropes and impacting it along the horizontal plane. Measurements of free-free mode natural frequencies and mode shapes are standard practice to assess the accuracy of the rotor structural model. The first measured and predicted natural frequency equal 196 Hz and 200 Hz, respectively. The second natural frequencies, test and prediction, occurs at 384 Hz and 443 Hz. The discrepancy is attributed to the mechanism locking the disks onto the shaft.[22]

Prior to the imbalance response experiments, the rotor is balanced in two planes. The resulting vibration due to the remnant imbalance is subtracted from the synchronous displacements measured with calibrated imbalances. Table 2 shows the specifications for the three test cases, each corresponding to a particular imbalance mass distribution. As mentioned above, each case requires two linearly independent imbalance tests. In the first test, the imbalance mass is placed in the drive-end disk only, and then this mass is removed and relocated on the free-end disk for the second test. Note that the values of imbalance used notably exceed common limits in industrial balancing practice (up to 36 times in the largest case), possibly corre-

CONTINUED ON PAGE 46

Table 1. Specifications of rotor-bearing system for the imbalance experiments

Shaft
$M_s = 6.69$ kg $L_s = 640$ mm $D_s = 25.4$ mm
$\rho_s = 7733$ kg/m^3 $E = 2.07 \times 10^{11}$ Pa

Disks (2 identical)
$M_d = 3.86$ kg each disk $D_d = 165$ mm $L_d = 32$ mm
Locations from the drive end $L_1 = 205$ mm, $L_2 = 485$ mm
Radius of attachment of imbalance mass $r_d = 70$ mm

Bearings (2-lobe type, 2 identical)
Bearing radial clearance $C_b = 0.092$ mm $L_b = 28.5$ mm $D_b = 25.4$ mm
Estimated dimensionless preload: 0.05

Location of bearing centerline from the sensor locations
Sensor 1 $s_1 = 40$ mm from bearing 1 (drive-end bearing)
Sensor 2 $s_2 = 23$ mm from bearing 2 (free-end bearing)

ISO VG 10 Lubricant
Average inlet lubricant temperature = 28^0C
Kinematic viscosity = 16.5 cSt
Kinematic viscosity at 40^0C = 10.4 cSt

Table 2. Specifications for the three test cases of imbalance measurements

Case	Imbalance mass m and angular location ϕ	Imbalance displacement, $u = m \times r_d / M_r$	Description
1	3.88 g @ 0^0	18.9 μm	Test 1 – u at drive-end disk
			Test 2 – u at free-end disk
2	7.25 g @ 0^0	35.3 μm	Test 1 – u at drive-end disk
			Test 2 – u at free-end disk
3	10.5 g @ 0^0	51.1 μm	Test 1 – u at drive-end disk
			Test 2 – u at free-end disk

Angles measured from key phasor mark on rotor. Radius of attachment r_d = 70 mm. Rotor mass M_r =14.4 kg. Allowable unbalance distance calculated at 4,500 rpm, from Eq. [1], = 1.41 μm.

CONTINUED FROM PAGE 45

Figure 2. Comparison of normalized responses recorded for different unbalance levels. Measurements at drive-end bearing and roto mid-span.

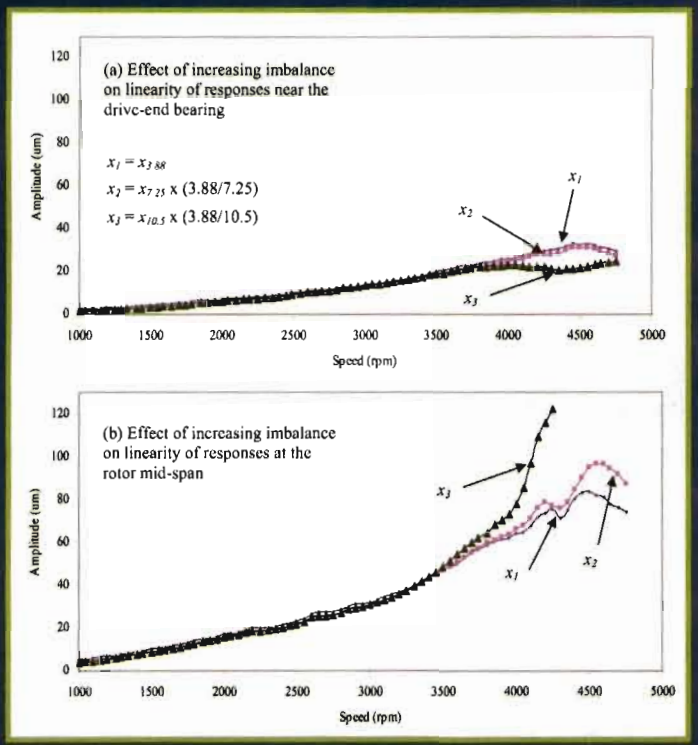

sponding to severe imbalance induced by process upsets, fouling or even detachment of internal components.

The test sequence is the following: in each run, the test rotor is brought up to a speed just above the first critical speed and then the motor power is shut off while the vibration measurements are cautiously recorded as the rotor decelerates to rest. Raw data obtained from the data acquisition contain synchronous amplitude and phase. The rotor synchronous amplitudes at the rotor mid-span are 40%-70% larger than the amplitudes near the bearing locations. Near the critical speeds, i.e., around 4500 rpm, the difference is larger (210 μm at *CY* and 60 μm at the free-end bearing in the vertical direction at same speed), more than 150%, reflecting the flexibility of the rotor. Phase angles for different values of imbalance remain almost the same over the shaft speed range shown.

The amplitude of rotor response at the drive-end bearing is larger than the response at the free-end bearing when an imbalance is placed in the drive-end disk. The maximum synchronous amplitudes near the two bearing locations are about 25 μm (26% of the bearing radial clearance) for an imbalance mass of 3.88 g, 55 μm (58 %) for an imbalance mass of 7.25 g, and 65 μm (70%) for the largest imbalance mass, 10.5 g.

For brevity, and in order to reveal the system linearity or lack thereof, Figure 2 presents the amplitudes of the rotor responses (*x* direction) at the rotor mid-span, due to the three combinations of imbalance mass, normalized to amplitudes recorded with an imbalance mass of 3.88 g. Critical speeds are observed for both cases of imbalance masses 3.88 g and 7.25 g at 4400 rpm and 4650 rpm, respectively. The critical speed was not reached for imbalance mass of 10.5 g because of large amplitudes of rotor motion at the bearing locations (70 μm), which are about 75% of the fluid film bearing radial clearances (93 μm).

The rotor-bearing system appears to behave linearly in the speed range from 2,200 rpm to 3,800 rpm, where the responses due to the higher imbalance mass can be thought of as a corresponding multiplication factor times the response due to a lower imbalance mass. As the shaft speed approaches the critical speed region (4200 rpm), the response amplitudes at the bearing locations due to greater imbalance masses are larger than the corresponding values the rotor would show if the system is regarded as linear. The test results do show a degree of non-linearity in the rotor response due to the large imbalance.

Equations of motion and method of identification

Figure 3. Schematic view of flexible rotor supported on anisotropic bearings.

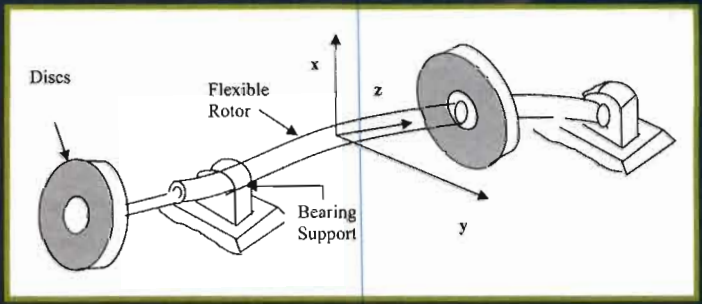

San Andrés and De Santiago[20] detailed the original method of support parameter identification in flexible rotors. The equations of motion for a generic flexible rotor-bearing system, as shown in Figure 3, are:

$$\mathbf{M\ddot{q}} + \mathbf{C\dot{q}} - \Omega\mathbf{G\dot{q}} + \mathbf{Kq} = \mathbf{Q(t)} \qquad (1)$$

where **M, C, G,** and **K** are the global matrices of inertia, damping, gyroscopic and stiffness coefficients, respectively. **Q** and **q** denote the vectors of generalized forces and displacements, and Ω represents the rotor speed. Using Timoshenko beam finite element matrices to model the rotating structure[15], with generalized vectors of dis-

placements and external forces from imbalance, suitable generalized stiffness and damping matrices result which contain the (yet unknown) bearing linearized force coefficients.

$$\mathbf{K}_{B_i} = \begin{bmatrix} K_{xx} & K_{xy} \\ K_{yx} & K_{yy} \end{bmatrix}_i ; \quad \mathbf{C}_{B_i} = \begin{bmatrix} C_{xx} & C_{xy} \\ C_{yx} & C_{yy} \end{bmatrix}_i \quad i = 1,2 \tag{2}$$

In general, $\mathbf{Q}(t) = \mathbf{Q}_u e^{i\omega t}$, and the rotor response has the same frequency as the excitation, i.e. $\mathbf{q}(t) = \mathbf{q}_u e^{i\omega t}$. Then, equations of motion (1) reduce to the algebraic form:

$$|\mathbf{K} - \omega^2\mathbf{M} + i\omega\mathbf{C} - i\,\omega\Omega\,\mathbf{G}|\,\mathbf{q}_u = \mathbf{Q}_u \tag{3}$$

In order to identify the unknown bearing coefficients, the algebraic system of Eq. (3) is reordered by use of matrix operations to yield

$$\mathbf{H}_{R(\omega\Omega)} \begin{Bmatrix} \mathbf{z}_{B_1} \\ \mathbf{z}_{B_2} \\ \mathbf{z}_{B_3} \end{Bmatrix} + \begin{bmatrix} \mathbf{H}_{B_1} & \mathbf{0} & \mathbf{0} \\ \mathbf{0} & \mathbf{H}_{B_1} & \mathbf{0} \\ \mathbf{0} & \mathbf{0} & \mathbf{0} \end{bmatrix} \begin{Bmatrix} \mathbf{z}_{B_1} \\ \mathbf{z}_{B_2} \\ \mathbf{z}_u \end{Bmatrix} = \begin{Bmatrix} \mathbf{0} \\ \mathbf{0} \\ \overline{\mathbf{Q}}_u \end{Bmatrix} \tag{4}$$

where

$$\mathbf{H}_{R(\omega\Omega)} = [\overline{\mathbf{K}}_R - \omega^2\overline{\mathbf{M}}_R + i\omega\overline{\mathbf{C}}_R - i\omega\Omega\,\overline{\mathbf{G}}] \tag{5}$$

is the dynamic rotor stiffness matrix (overbars denote the reordered matrix),

$$\mathbf{H}_{B_1} = \mathbf{K}_{B_1} + i\omega\,\mathbf{C}_{B_1} ; \; \mathbf{H}_{B_2} = \mathbf{K}_{B_2} + i\omega\mathbf{C}_{B_2} \tag{6}$$

represent the supports impedance (dynamic stiffness) matrices, and ($\mathbf{z}_{B_1}$, $\mathbf{z}_{B_2}$) are the motions at the bearing support locations. The generalized load vector $\mathbf{Q}_u$ is known from the imbalance distribution, while the vector $\mathbf{z}_u$ represents the vector of unknown rotor displacements. These rotor displacements are not observable or measured, but are readily computed using the measured displacements at the bearing locations and adequate submatrices of the rotor impedance matrix $\mathbf{H}_R$

Using suitable submatrices of the rotor dynamic stiffness matrix $\mathbf{H}_R$, bearing transmitted forces ($\mathbf{f}_{B1}$, $\mathbf{f}_{B2}$) are readily defined as:

$$\begin{aligned} \mathbf{H}_{B_1}\mathbf{z}_{B_1} &= -\mathbf{H}_{R11}\mathbf{z}_{B_1} - \mathbf{H}_{R12}\mathbf{z}_{B_2} - \mathbf{H}_{R13}\mathbf{z}_u = \mathbf{f}_{B_1} \\ \mathbf{H}_{B_2}\mathbf{z}_{B_2} &= -\mathbf{H}_{R21}\mathbf{z}_{B_1} - \mathbf{H}_{R22}\mathbf{z}_{B_2} - \mathbf{H}_{R23}\mathbf{z}_u = \mathbf{f}_{B_2} \end{aligned} \tag{7}$$

In Eq. (7), the submatrices $\mathbf{H}_{R11}$, $\mathbf{H}_{R12}$,... only contain parameters belonging to the rotating structure, and not to the bearing supports. Each of these equations represents two algebraic equations (x, y). However, the number of (complex) bearing parameters is four at each support location. Experimentally, two (known) mass imbalances at selected rotor positions will produce two rotor responses. The imbalance distributions $|(m,u,\phi)_k|_{j=1,2}$ must be such that they render linearly independent rotor responses. The displacements at the bearing supports are $\{\mathbf{z}_{B11}, \mathbf{z}_{B21}\}$ and $\{\mathbf{z}_{B12}, \mathbf{z}_{B22}\}$; with corresponding reaction forces $\{\mathbf{f}_{B11}, \mathbf{f}_{B21}\}$ and $\{\mathbf{f}_{B12}, \mathbf{f}_{B22}\}$. With this information, the support impedance coefficients are determined by solving:

$$\mathbf{H}_{B_1} = \begin{bmatrix} K_{xx} + i\omega C_{xx} & K_{xy} + i\omega C_{xy} \\ K_{yx} + i\omega C_{yx} & K_{yy} + i\omega C_{yy} \end{bmatrix}_{B_1} = |\mathbf{f}_{B11} \;\; \mathbf{f}_{B21}|\;|\mathbf{z}_{B11}, \mathbf{z}_{B21}|^{-1} \tag{8}$$

for bearing support 1. A similar equation arises for bearing support 2. When measurements of rotor response are not taken exactly at the bearing locations (as it often happens in actual system configurations), the use of interpolation functions relating the motions at the ends of the element containing the point of measurement allows estimation of the displacements at the bearing locations, as:

$$\begin{aligned} \mathbf{z}_{B1} &= a\,\mathbf{z}_{m1} + \mathbf{A}\,\mathbf{z}_u \\ \mathbf{z}_{B2} &= b\,\mathbf{z}_{m2} + \mathbf{B}\,\mathbf{z}_u \end{aligned} \tag{9}$$

where $\mathbf{z}_{m1}$ and $\mathbf{z}_{m2}$ are the measured response vectors *near* the bearing locations (at the location of sensors), a and b are the known scalar functions of the interpolation functions and **A** and **B** are the matrix functions of the interpolation functions. The development then continues as before to find the bearing forces as:

$$\begin{aligned} -\mathbf{f}_{B1} &= a\,\mathbf{H}_{R11}\,\mathbf{z}_{m1} + b\,\mathbf{H}_{R12}\,\mathbf{z}_{m2} + \overline{\mathbf{H}}_{R13}\,\mathbf{z}_u \\ -\mathbf{f}_{B2} &= a\,\mathbf{H}_{R21}\,\mathbf{z}_{m1} + b\,\mathbf{H}_{R22}\,\mathbf{z}_{m2} + \overline{\mathbf{H}}_{R23}\,\mathbf{z}_u \end{aligned} \tag{10}$$

and from there, bearing impedance estimates are easily obtained by writing Eqs. (10) as:

$$\mathbf{H}_B\mathbf{DM} = \mathbf{RF} \tag{11}$$

where **DM** and **RF** are measured data matrices and reactive force matrices formed by augmenting the two equations of (10) from two consecutive imbalance tests. Each bearing impedance matrix is then readily obtained by:

$$\mathbf{H}_B = \mathbf{RF}\,\mathbf{DM}^{\dagger} \tag{12}$$

where the cross symbol represents either the inverse operation or a pseudo-inverse operator suitable for overdetermined systems (i.e., when there are redundant imbalance runs available for identification).

Identified bearing support parameters

The identification procedure uses the recorded rotor responses (*see Figure* 2) for the three cases of mass imbalance to determine the bearing stiffness and damping coefficients. The only requirement for the enhanced identification procedure is that the rotor model has finite elements nodal dispositions at the bearing locations. Recall that the test rotor is supported on two identical bearings;

CONTINUED ON PAGE 48

Figure 4. Identified rotordynamic force coefficients of two-lobe bearing. Identification from measurements with an imbalance mass of 3.88 g.

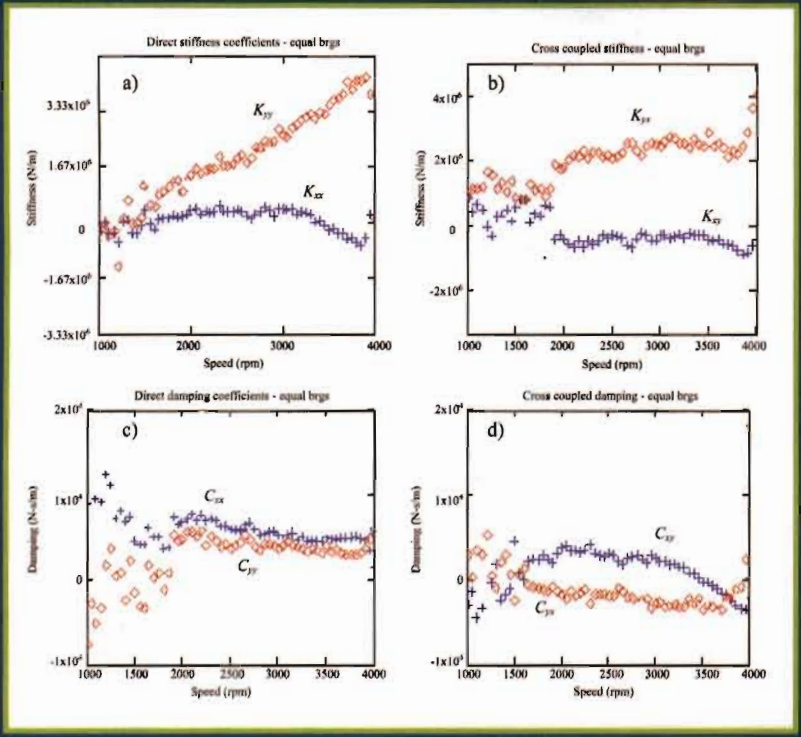

Figure 5. Identified rotordynamic force coefficients of two-lobe bearing. Identification from measurements with an imbalance mass of 7.25 g.

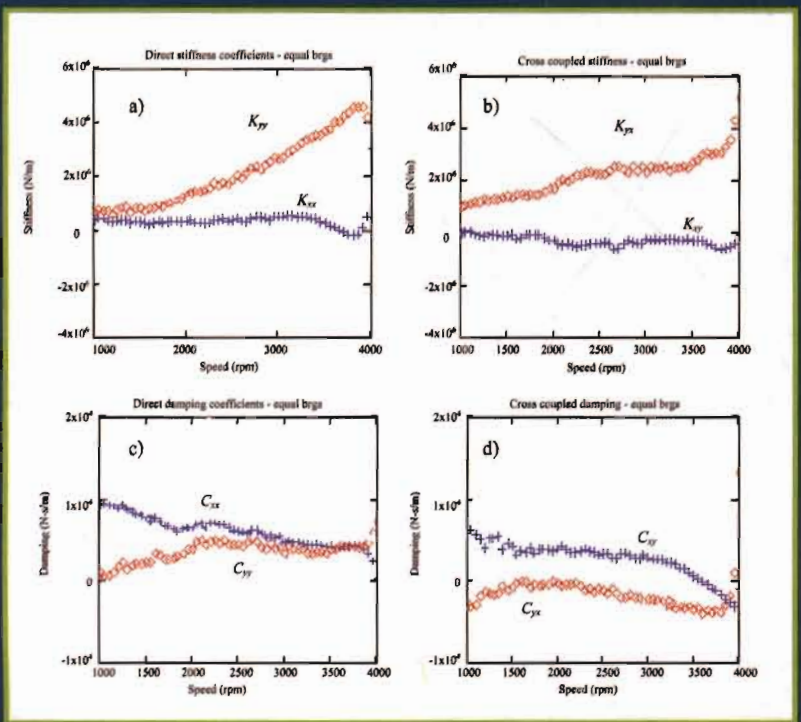

CONTINUED FROM PAGE 47

thus it is reasonable to expect that the bearings have similar dynamic force coefficients since both of them carry similar static loads and operate at similar static journal eccentricities. Assuming that the bearings have identical dynamic force coefficients also reduces the number of unknowns from sixteen to eight. The least squares procedure is then implemented to identify the bearing dynamic force coefficients.

In the following, it is important to note that the test bearings have uneven wear around their inner surfaces (axial and circumferential), making difficult the exact determination of the actual preload. The test bearings thus may represent a commercial application after a considerable period of usage. These facts prevent the accurate prediction of bearing force coefficients, and thus the investigation presented here is only experimental and no comparison with predicted values is presented.

Figures 4 to 6 depict the estimated bearing dynamic force coefficients from measured responses for three increasing imbalance masses for the two-lobe test bearings. Similar patterns of bearing coefficients are observed from all the three increasing imbalance mass excitations. The direct stiffness coefficients (K_{xx}, K_{yy}) are similar at low shaft speeds and then K_{yy} increases, whereas K_{xx} remains almost constant throughout the identification speed range. At low speeds, damping coefficients are larger in the horizontal direction (C_{xx}) than in the vertical direction (C_{yy}) and as the speed approaches 2400 rpm and from thereon, the damping coefficients remain nearly invariant.

The cross-coupled stiffness coefficient (K_{xy}) is negative and decreases slightly as the identification speed increases, whereas the other cross-coupled stiffness coefficient (K_{yx}) is positive and increases slowly over the speed range considered. Note that the cross-coupled stiffness coefficients are of opposite sign, indicating the presence of a follower force in the two-lobe cylindrical bearings. Cross-coupled damping coefficients are smaller than the direct damping

coefficients and are of opposite sign.

Ill conditioning happens often in engineering problems and is usually related to the elements of a matrix with very different magnitudes from each other. The matrix condition number (CN), defined as the product of the Euclidean norm of a matrix **A** and $\mathbf{A}^{-1}$, provides a measure of the sensitivity of the linear system of equations to variations in the elements of **A**, due to noise or uncertainty in measurements. A large value of the condition number implies that the measurement data matrix is ill conditioned and propagates errors in the calculation of its inverse to obtain the bearing parameters.[18]

Recall that during the identification process a system of equations results (Eqs. (8) or (11)). The measurement data matrix changes as a function of speed and so does its condition number. Figure 7 shows this condition number of the measurement data matrix for the three imbalance test cases. For a low imbalance mass (3.88 g), the condition number is higher than the corresponding CNs of the identification matrices for higher imbalance masses at shaft speeds less than 2000 rpm. Note that 3.88 g imbalance mass gives good coefficients in the speed range of 2.0 to 3.5 krpm. Large values of the condition number for shaft speeds greater than 3800 rpm indicate numerical ill- conditioning and results in unreliable (poor) identified coefficients in the noted speed range. Notice that the amplitudes of vibration for 3.88 g of imbalance mass excitation are small compared to the responses from large imbalance mass (7.25 g and 10.5 g) excitations. Thus, it is likely that the measurements from small imbalances are affected by noise resulting in poor identification when compared to the identification results from 7.25 g and 10.5 g imbalance mass excitations.

At the rotor critical speeds, ~ 4,000 rpm, the CN for all the test cases increases up to 15 times the average value; thus slight errors in the measurement of rotor response near the critical speeds largely affect the accuracy of the identified bearing coefficients. Numerous peaks in the condition number for the case of 3.88 g of imbalance mass at low rotational speeds, i.e., below 2000 rpm, explains

CONTINUED ON PAGE 50

Figure 6. Identified rotordynamic force coefficients of two-lobe bearing. Identification from measurements with an imbalance mass of 10.5 g.

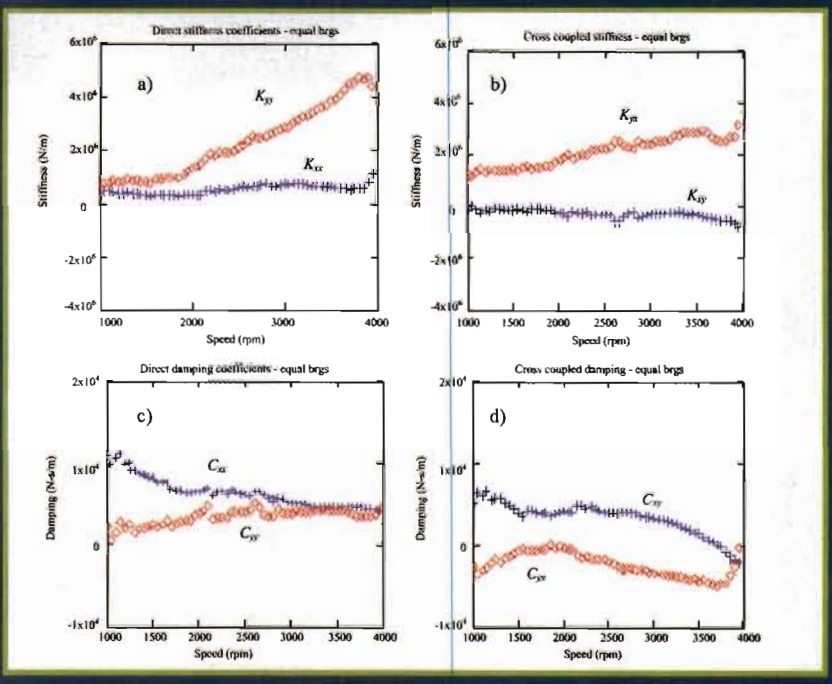

Figure 7. Condition number of the quadratic form of the measurement data matrix for all test cases (identification response matrix) as a function of identification speed.

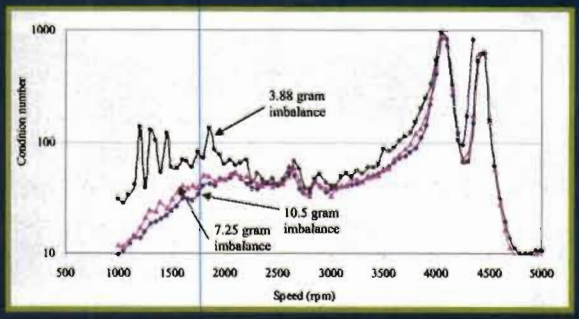

Figure 8(a). Identified rotordynamic force coefficients from imbalance mass excitation of 10.5 g. Identification after the inclusion of Gaussian noise, NSF = 1%, in the recorded responses.

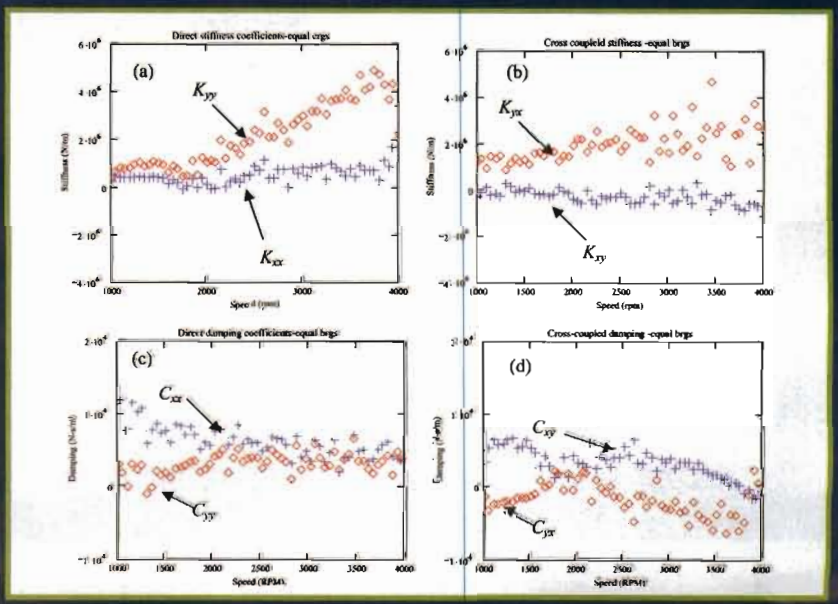

Figure 8(b). Identified rotordynamic bearing coefficients from imbalance mass excitation of 10.5 g. Identification after the inclusion of Gaussian noise, NSF = 10%, in the recorded responses.

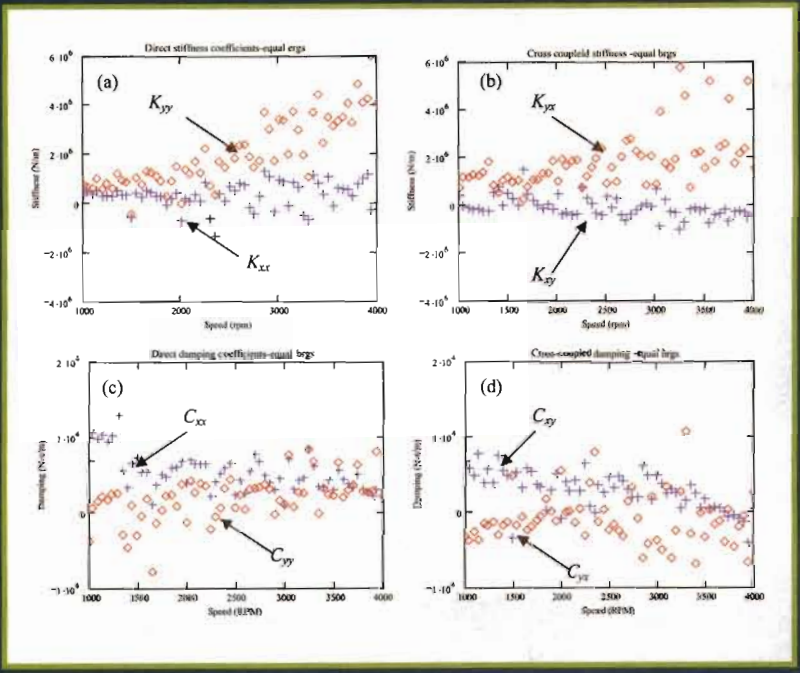

Figure 9. Bearing force coefficients estimated from measurements of 10.5 g imbalance. Original and enhanced identification methods. Lines represent original identification, symbols represent enhanced identification.

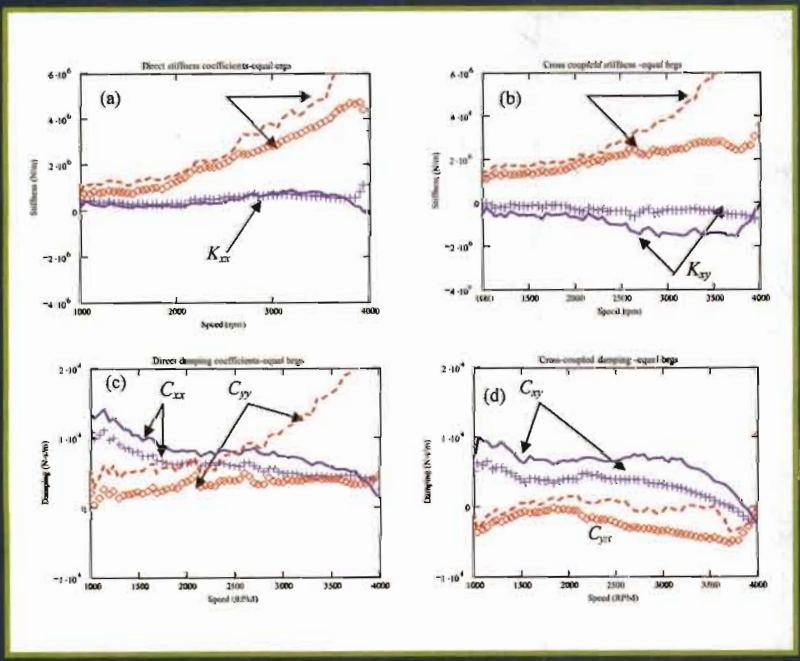

CONTINUED FROM PAGE 49

the reason for the scatter of identified coefficients, particularly for damping coefficients. This attests for the few negative values of damping coefficients, which are not feasible in stable systems.

Returning to Figures 4 thru 6, the bearing direct stiffness coefficients increase with the amount of imbalance excitation used to determine those coefficients. The direct stiffness coefficients (K_{uu}) estimated from 10.5 g imbalance mass excitation are on average 7% larger compared to the corresponding coefficients obtained from 3.88 g imbalance mass excitation. The direct stiffness coefficients (K_{xx}) are 20% larger for the same comparison of imbalance cases. The direct stiffness (K_{xx}) identified from an imbalance mass excitation of 3.88 g are negative at the operating speed of 4000 rpm, due to the ill-conditioning of the measured data matrices explained by high values of condition number matrices at those speeds.

The direct damping coefficients (C_{xx}) identified from imbalance mass of 10.5 g, are on average 6% larger when compared to the coefficients determined from 7.25 g imbalance. A similar increase is observed in the other direct damping coefficient (C_{yy}). Thus, the bearing direct coefficients are found to increase with the amount of imbalance mass.

The cross-coupled coefficients are found to increase in magnitude although the trend is not as well defined as with the bearing direct coefficients. For a 40% increase in the imbalance mass, cross-coupled damping coefficients (C_{xy}) are 20% larger. The cross-coupled damping coefficients (C_{yx}) are negative in the speed range considered and, on average 23% larger in magnitude for that increase in the imbalance mass.

The identification of bearing synchronous coefficients from various imbalance mass excitations shows the procedure is most sensitive to the smallest imbalance mass (3.88 g). All the bearing synchronous force coefficients increase with the amount of imbalance mass. The identification method is robust for the case of large

imbalance mass excitation (10.5 g), which provides reliable results of bearing force coefficients. Identified coefficients are scattered at low speeds for lower imbalances where the sensitivity of the algorithm to the presence of noise is large, as is shown next.

Balantrapu and San Andrés[22] also discuss the effect of increasing the number of elements in the rotor model. The result is that a too fine finite element discretization of rotor shaft is not a crucial factor in the accuracy of the identified bearing dynamic coefficients (identified values remaining within 3% to 4% for up to 2.5 times more elements in the rotor model).

Effect of noise on identified force coefficients

Measurement data is always contaminated by different types of noise; be it from mechanical or electrical instrumentation. The least squares procedure for estimating bearing dynamic coefficients has a bias problem whenever noise is included in the measurement data matrix.[23] Hence it is worthwhile studying the effect of noise on the identified bearing coefficients.

The noise-to-signal ratio (NSR) is defined as

$$\mathbf{NSR} = \frac{\mathbf{STD}\ [\text{noise}]}{\mathbf{STD}\ |x_0|} \qquad (13)$$

where STD is a standard deviation, and x_0 is the measurement value. Gaussian noise, NSR = 1% and 10%, is added to the measurements for 10.5 g imbalance and bearing dynamic coefficients re- estimated. Figure 8 depicts the results obtained with identified bearing coefficients following the trend of the baseline coefficients identified without inclusion of noise (*see Figure 6*). Large differences of about 130% in cross-coupled stiffness values for 10% inclusion of NSR are apparent. Direct stiffness coefficients are almost invariant to the largest inclusion of noise-to-signal ratio (10%), the variation being 10%-15% from the identified values.

Note also that the bearing coefficients identified for the case of NSR=10% differ most with the baseline coefficients at shaft speeds (> 4000 rpm) where the condition number of the measurement data matrix **DM** shows the largest magnitudes. Also notice that a few direct damping coefficients are negative with the inclusion of noise. Identification of bearing dynamic force coefficients thus requires accurate measurement of phase angles and amplitudes of rotor responses.

For the largest imbalance test case (10.5 g), the bearing force coefficients were estimated in San Andrés and De Santiago[20] and assuming the rotor response measurements were obtained at the bearing centerline locations. Figure 9 shows the earlier bearing force coefficients and the present bearing coefficients identified from 10.5 g imbalance mass (*see Figure 6*). The direct stiffness coefficient $K_{\alpha\alpha}$ shows no significant variation with the original method. The other direct stiffness coefficient $K_{\beta\beta}$ differs by 10% on average. The differences in the bearing force coefficients, estimated from the two procedures, increase at large shaft speeds, except for the direct damping coefficient ($C_{\alpha\alpha}$).

Conclusions

A procedure is presented, along with its experimental implementation, for identification of bearing synchronous force coefficients in flexible rotor-bearing systems over an operating speed range. The proposed identification method enhances the original method (San Andrés and De Santiago[20]) by recognizing that in practice the measurement locations (eddy-current displacement sensors) do not coincide with the bearing centerline locations. Realistic bearing parameters as a function of rotor speed are necessary for predictions of rotor response to imbalances.

Assumption of identical bearings in reducing the number of unknowns is justified by the physical arrangement of the rotor-bearing system. The identification by imbalance response measurements is largely influenced by shaft flexibility as confirmed by the deflections at rotor mid-span.

Bearing force coefficients are identified for three different imbalance mass excitations. The effect of the imbalance mass amount, used for system excitation, on the identified coefficients is found to be mild. Insignificant differences are observed for identification from different values of imbalance masses, except with the lowest imbalance mass. An optimum amount of imbalance needs to be selected for identification such that the rotor responses are large enough to ensure low noise-to-signal ratios. In particular, the identification of bearing parameters from imbalance responses is quite sensitive at rotor critical speeds (rapid phase angle changes), although large rotor amplitudes at those speeds minimize the noise-to-signal ratio.

The sensitivity of the procedure to the presence of noise in the measurements is assessed by incorporating 1% and 10% Gaussian noise in the responses and identifying the bearing dynamic force coefficients. The extracted bearing parameters do not vary significantly, which attests to the robustness of the identification procedure.

Acknowledgements

The support of the Turbomachinery Research Consortium at Texas A&M University is acknowledged. <<

CONTINUED ON PAGE 52

CONTINUED FROM PAGE 51

References

(1) American Petroleum Institute Standard 617. (2002), "Axial and Centrifugal Compressors and Expander-Compressors for Petroleum, Chemical and Gas Industrial Services—7th Edition," Washington D.C., July.

(2) American Petroleum Institute Standard 541. (2003), "Form-wound Squirrel-Cage Induction Motors—500 Horsepower and Larger—4th Edition," Washington D.C., June.

(3) American Petroleum Institute Standard 546. (1997), "Brushless Synchronous Machines—500 kVA and Larger—2nd Edition," Washington D.C., June.

(4) American Petroleum Institute Standard 613. (1995), "Special Purpose Gear Units For Petroleum, Chemical, And Gas Industry Services—4th Edition," Washington D.C., June.

(5) Goodwin, M.J. (1991), "Experimental Techniques for Bearing Impedance Measurement," ASME *Journal of Engineering for Industry*, **113**, Aug., pp. 335-342.

(6) Morton, P.G. (1971), "Measurement of the Dynamic Characteristics of a Large Sleeve Bearing," *Journal of Lubrication Technology*, **79**, pp. 143-150.

(7) Nordmann, R. and Schollhorn, K. (1980), "Identification of Stiffness and Damping Coefficients of Journal Bearings by Means of the Impact Method," *Proceedings of the International Conference on Vibration in Rotating Machinery* (ISROMAC), IMechE, Cambridge, England, pp. 231-238.

(8.) De Santiago, O. and San Andrés, L. (2007), "Field Methods for Identification of Bearing Support Parameters. Part I—Identification from Transient Rotor Dynamic Response Due to Impacts," ASME *Journal of Engineering for Gas Turbines and Power*, **129**, pp. 205-212.

(9) Burrows, C.R., and Sahinkaya, M.N. (1982), "Frequency-Domain Estimation of Linearized Oil-Film Coefficients," *Journal of Lubrication Technology*, **104**, pp. 210-215.

(10) Lee, C.W., and Hong, S.W. (1989), "Identification of Bearing Dynamic Coefficients by Imbalance Response Measurements," *Proc. Inst. Mech. Engrs.*, **203**, pp. 93-101.

(11.) De Santiago, O. and San Andrés, L. (2007), "Field Methods for Identification of Bearing Support Parameters. Part II—Identification from Rotordynamic Response due to Imbalances," ASME *Journal of Engineering for Gas Turbines and Power*, **129**, pp. 213-219.

(12) Ruhl R.L., and Booker, J.F. (1972), "A Finite Element Model for Distributed Parameter Turbo Rotor Systems," ASME *Journal of Engineering for Industry*, **68**, pp. 128-132.

(13) Nelson, H.D, and McVaugh, J.M. (1976), "The Dynamics of Rotor-Bearing Systems Using Finite Elements," ASME *Journal of Engineering for Industry*, **98** (2), pp. 593-600.

(14) Zorzi, E.S., and Nelson, H.D. (1977), "Finite Element Simulation of Rotor-Bearing Systems with Internal Damping," ASME *Journal of Engineering for Power*, **99** (1), pp. 71-76.

(15) Nelson, H.D. (1980), "A Finite Rotating Shaft Element Using Timoshenko Beam Theory," ASME *Journal of Mechanical Design*, **102** (4), pp. 793-803.

(16) Chen, J.H., and Lee, A.C. (1997), "Identification of Linearized Dynamic Characteristics of Rolling Element Bearings," ASME *Journal of Vibration and Acoustics*, **119**, pp. 60-69.

(17) Burrows, C.R., and Stanway, R. (1977), "Identification of Journal Bearing Characteristics," *Trans.* ASME, J. *Dynamic Systems Measurement and Controls*, **99**, pp. 167-173.

(18) Murphy, B.T., Scharrer, J.K., Sutton, R. (1990), "The Rocketdyne Multifunction Tester, Part I: Test Method." Workshop on Rotordynamic Instability Problems in High Performance Turbomachinery, Texas A&M University, May.

(19) Yang T., and Chaung W.C. (2000), "Identification of Bearing Coefficients of Flexible Rotor-Bearing Systems," ASME paper 2000 GT-400.

(20) San Andrés, L., and De Santiago, O. (2004), "Identification of Bearing Force Coefficients from Measurements of Imbalance Response of A Flexible Rotor," ASME Paper GT2004-54160.

(21) Tiwari, R., Lees, A.W., and Friswell, M.I. (2004), "Identification of Dynamic Bearing Parameters: a Review," *The Shock and Vibration Digest*, March, **36** (2), pp. 99-124.

(22) Balantrapu, K., and San Andrés, L. (2004), "Identification of Force Coefficients in Flexible Rotor-Bearing Systems—Enhancements And Further Validations," Technical Report TRC-B&C-1-04, Turbomachinery Laboratory, Texas A&M University, May.

(23) Fritzen, C. (1986), "Identification of Mass, Damping and Stiffness Matrices of Mechanical Systems," ASME *Journal of Vibration, Acoustics, Stress and Reliability in Design*, **108** (1), pp. 9-16.